Cluster structure prediction in USPEX: basics, examples and recent developments

Vladimir Baturin

RSF Russian Science Foundation

Skoltech
Skolkovo Institute of Science and Technology

ФЕДЕРАЛЬНОЕ ГОСУДАРСТВЕННОЕ БЮДЖЕТНОЕ УЧРЕЖДЕНИЕ НАУКИ
Физический институт имени П.Н.Лебедева
РОССИЙСКОЙ АКАДЕМИИ НАУК
Ф И А Н

Contents

1. New variable-composition method for cluster structure prediction
2. Application to Si_nO_m clusters in wide area of compositions: $1 \le n \le 15$, $0 \le m \le 20$
3. Charge trapping in Cd_nSe_m clusters

Fixed composition cluster structure prediction

Theoretical structure prediction of nanoclusters is a very complicated problem:

1. A large number of atoms in a cluster to consider
2. In most cases the real cluster structure differs from the model structures either cut from bulk lattice or built considering some point symmetry. Low symmetry of the system is possible
3. The experimental data on the structure of nanoclusters is also very limited

Fixed composition cluster structure prediction

In the current version the **000** method is available

1. 1-st generation is initialized randomly, with clusters obeying one of 32 crystal point group plus some important non-crystallic point groups:

Crystallographic point groups:

Hermann-Maugin	Schönflies	In USPEX
1	C_1	C1 or E
2	C_2	C2
222	D_2	D2
4	C_4	C4
3	C_3	C3
6	C_6	C6
23	T	T
$\bar{1}$	S_2	S2
M	C_{1h}	Ch1
mm2	C_{2v}	Cv2
$\bar{2}$	S_4	S4
$\bar{3}$	S_6	S6
$\bar{6}$	C_{3h}	Ch3
m$\bar{3}$	T_h	Th
2/m	C_{2h}	Ch2
mmm	D_{2h}	Dh2
4/m	C_{4h}	Ch4
32	D_3	D3
6/m	C_{6h}	Ch6
432	O	O
422	D_4	D4
3m	C_{3v}	Cv3
622	D_6	D6
$\bar{4}$3m	T_d	Td
4mm	C_{4v}	Cv4
$\bar{3}$m	D_{3d}	Dd3
6mm	C_{6v}	Cv6
m$\bar{3}$m	O_h	Oh
$\bar{4}$2m	D_{2d}	Dd2
$\bar{6}$2m	D_{3h}	Dh3
4/mmm	D_{4h}	Dh4
6/mmm	D_{6h}	Dh6
m$\bar{3}$m	O_h	Oh

Important non-crystallographic point groups

Hermann-Maugin	Schönflies	In USPEX
5	C_5	C5
5/m	S_5	S5
$\bar{5}$	S_{10}	S10
5m	Cv_{5v}	Cv5
$\bar{10}$	Ch_{5h}	Ch5
52	D_5	D5
$\bar{5}$m	D_{5d}	Dd5
$\bar{10}$2m	D_{5h}	Dh5
532	I	I
5$\bar{3}$m	I_h	Ih

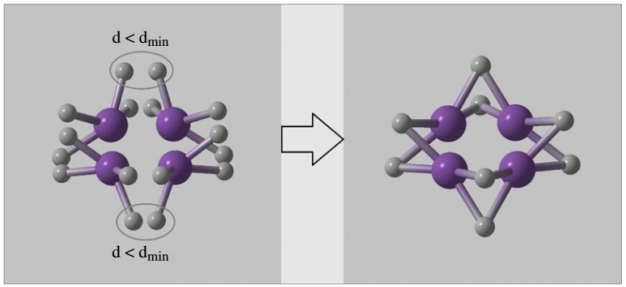

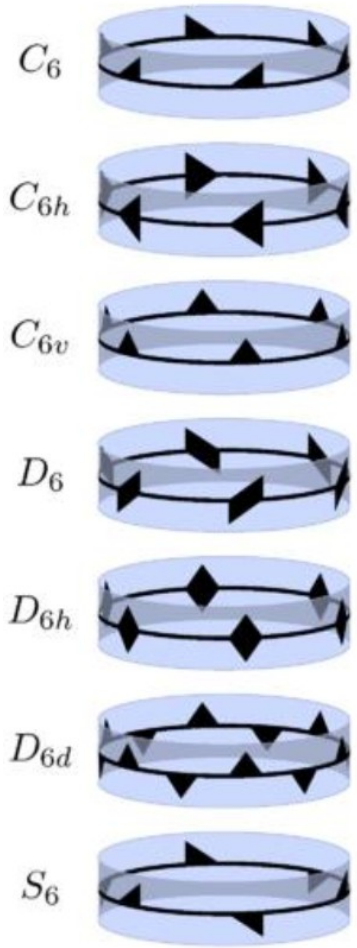

Fixed composition cluster structure prediction

2. The following generations are produced via similar operators to 3D, but with some important differences

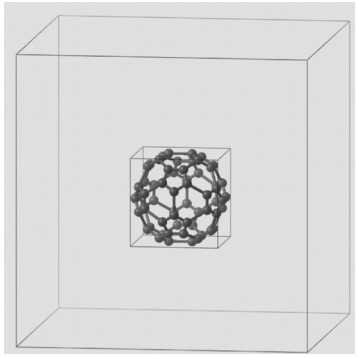

1. Usually supercell approach is applied
2. In that case all variation operators are applied to the “small cell”
3. The fingerprint vector is changed:

$$F_{A_iB}(R) = \sum_{B_j} \frac{\delta(R - R_{ij})}{4\pi\, R_{ij}^2 N_B \Delta}$$

4. Slab-by-slab heredity is replaced by the cut-and-splice operator

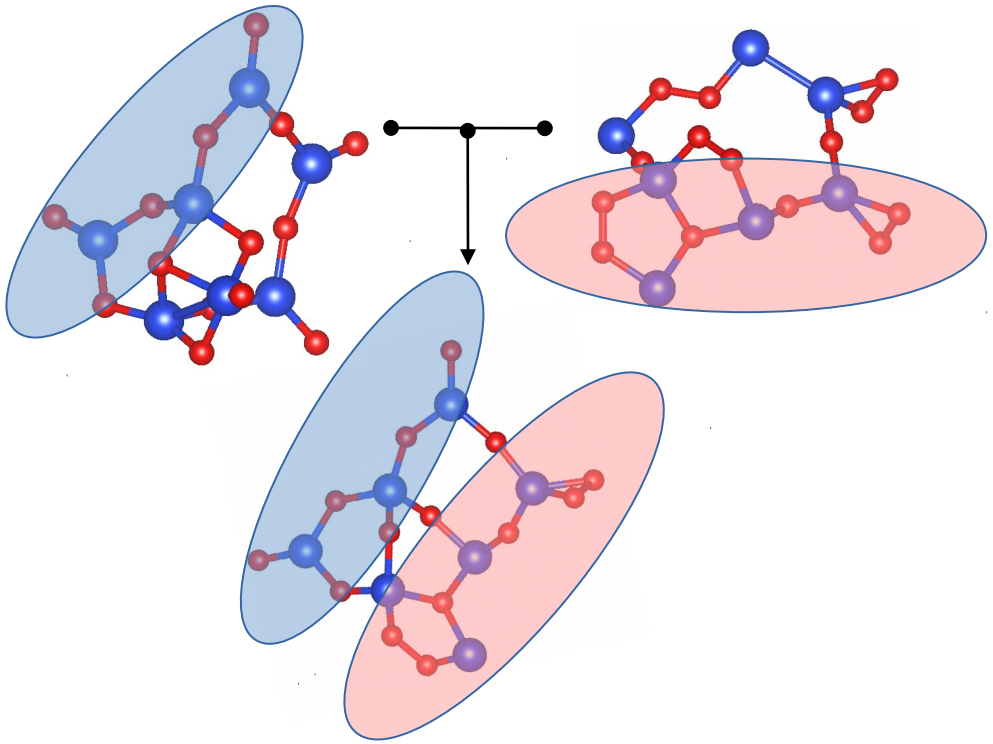

For practical applications tens or hundreds of cluster compositions should be considered:

- in experiments clusters are often formed as ensembles of various sizes and compositions
- to study nucleation processes;
- to find compounds with required properties;
- etc.

The computation of *N* different cluster compositions is *N* times longer than one individual foxed-composition calculation.

New method: New search space, new fitness function, new variation operators

1. New search space – the union of search spaces of clusters with different compositions from a user-defined range:

```
% atomType
Cu Au
% EndAtomType
% numSpecies
6 10
6 10
% EndNumSpecies
```

New method: New search space, new variation operator, new fitness function

New fitness function:

Total energy doesn't work

The only thermodynamically stable cluster is an infinite one, i.e. bulk → cohesion, reaction, formation or binding energy don't work either

The solution is to exploit the idea of the **magic clusters** – the most abundant in nature and in the mass spectra of particle beams

Stability of the clusters: magic clusters

Model system: Lennard-Jones clusters

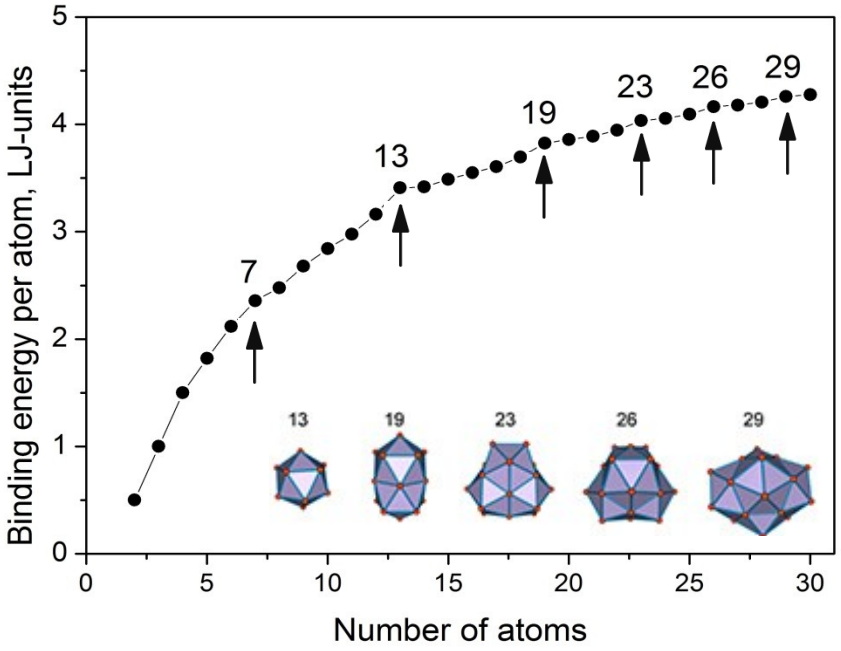

↑ – magic clusters

Real system: Pb clusters

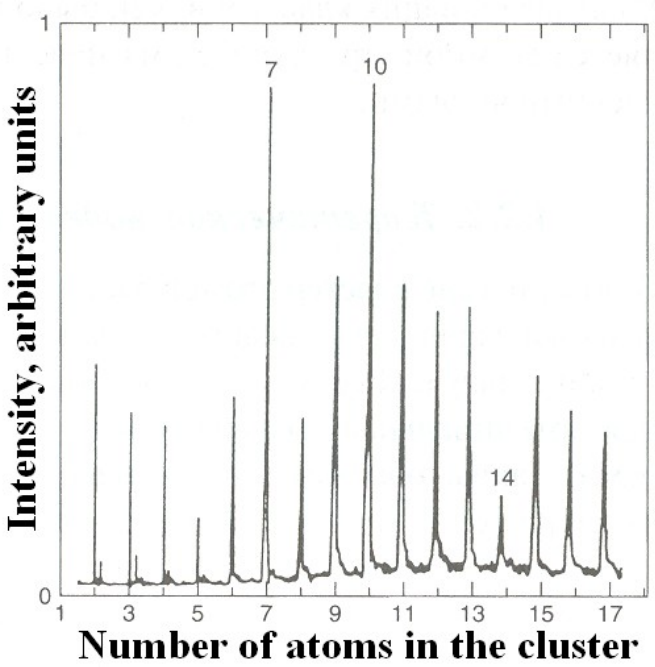

mass spectrum of $(Pb)_n$ clusters (Poole & Owens, 2003)

For clusters, stability can be determined with respect to neighboring clusters

Magic clusters

Model system: Lennard-Jones clusters

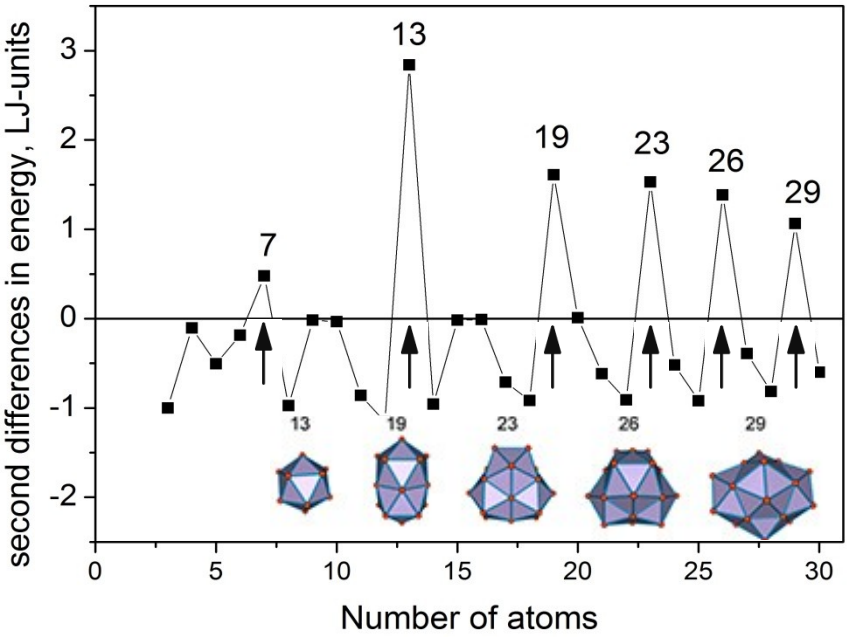

↑ – magic clusters

Real system: Pb clusters

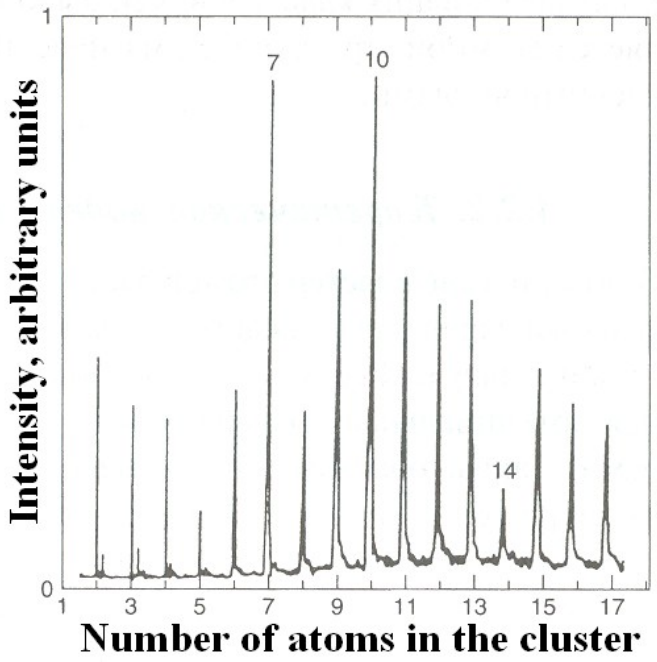

mass spectrum of $(Pb)_n$ clusters (Poole & Owens, 2003)

Stability criterion (magic clusters):

$$\Delta^2 E = E(n+1) + E(n-1) - 2E(n) > 0, \text{ or}$$
$$E(n) < (E(n+1) + E(n-1))/2$$

Method: computational scheme; choosing the target function of optimization

New fitness – energy is counted with respect to a line connecting neighboring magic clusters

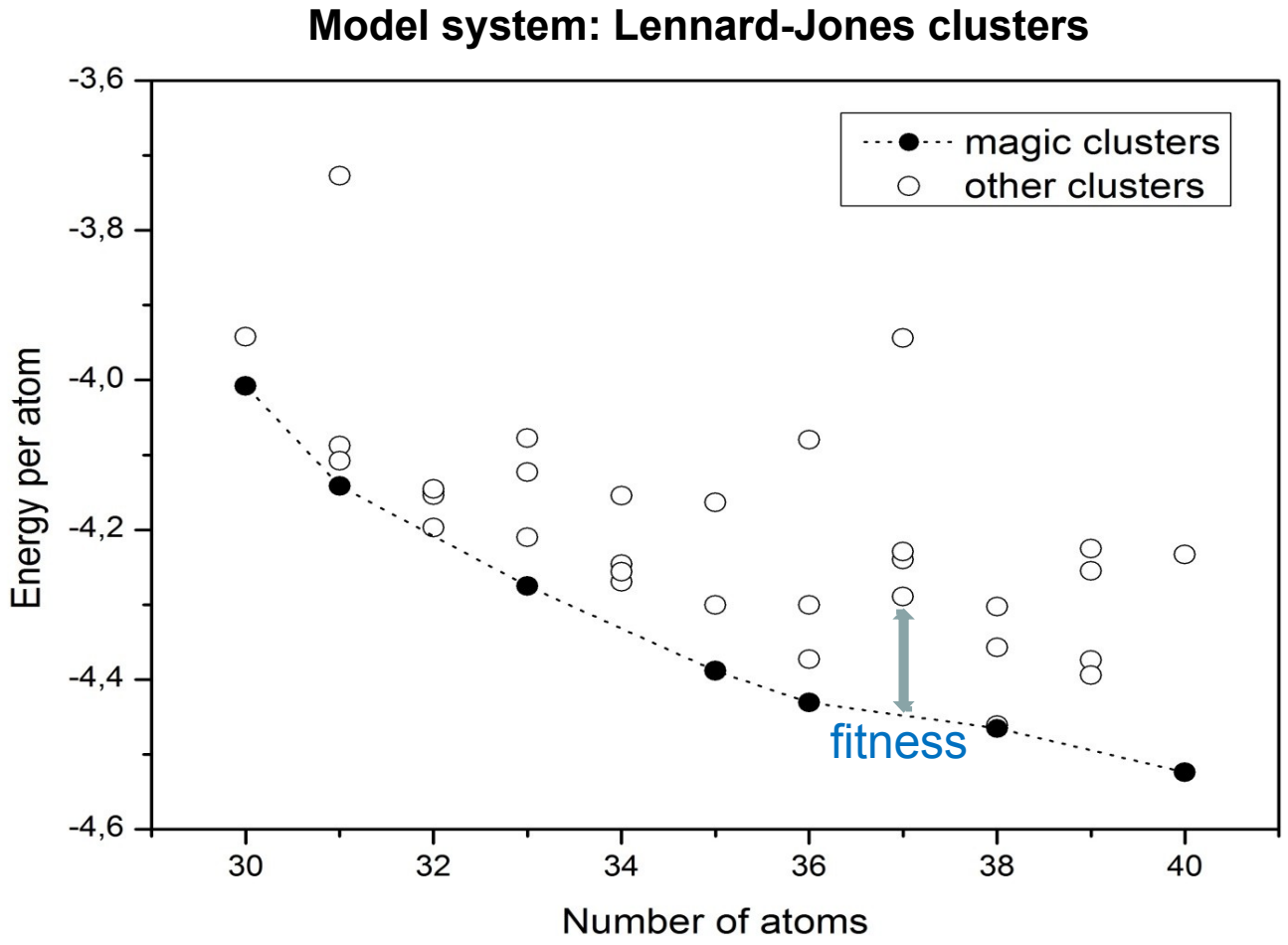

Method: variation operators

Operators in the standard fixed-composition mode:

- Random initialization
- Heredity (parents and offspring of the same composition)
- Softmutation
- Permutation

New operators in the variable-composition mode:

- Transmutation
- New heredity (parents may have different compositions)
- Add or remove atom

Add and remove atom

Coordination numbers: $o_i = \frac{\sum_j (\exp(-(\Delta r_{ij} - R_i - R_j)/0.37))}{max(\exp(-(\Delta r_{ij} - R_i - R_j)/0.37))}$

R_i - covalent radius of atom i:

Probability of addition or removal atom (for every type of atom):

$p_i \sim o_{i\,max} - o_i$

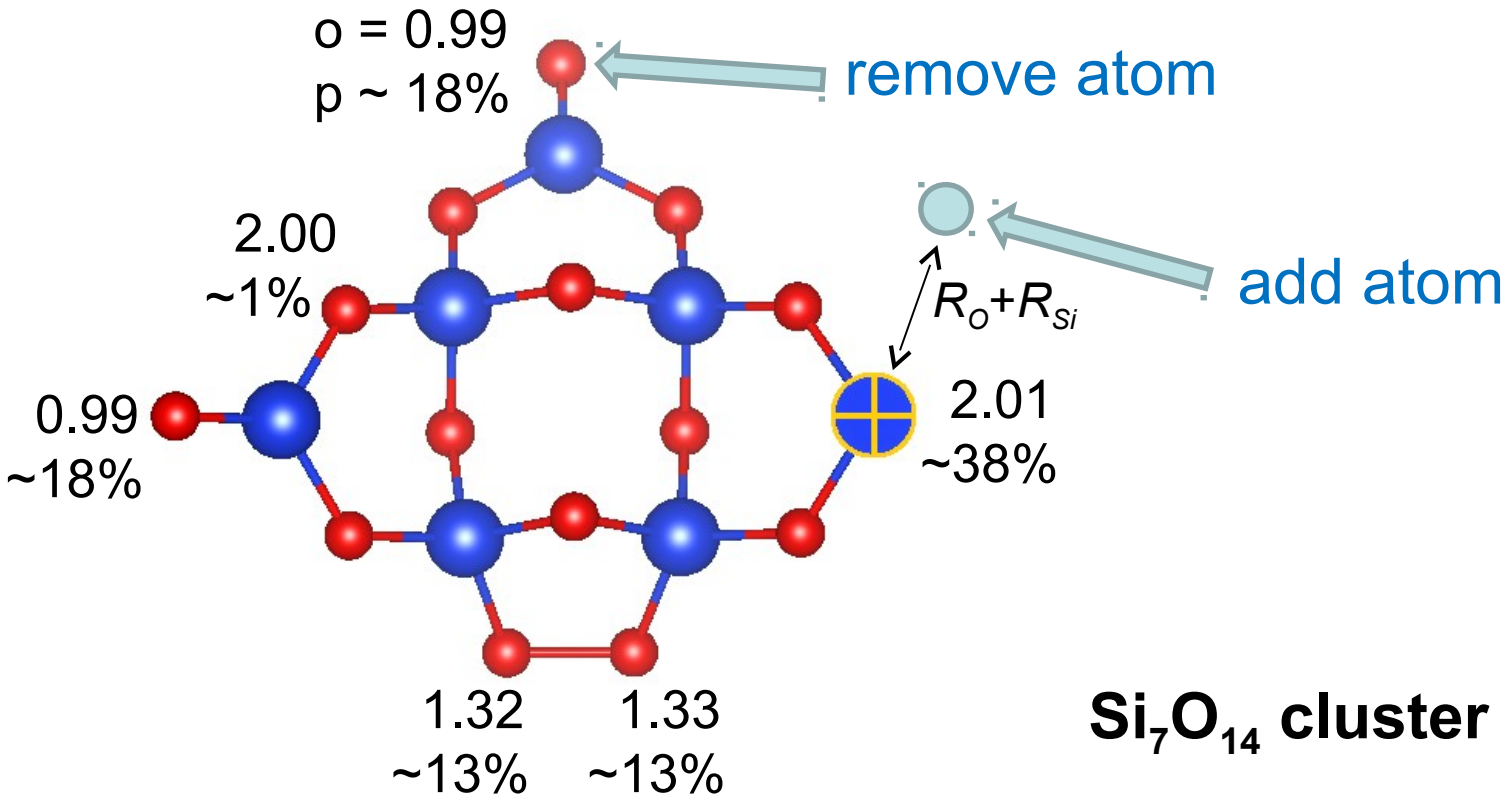

Si_7O_{14} cluster

Variable-composition vs. fixed-composition

Model system: Lennard-Jones clusters with 30-60 atoms

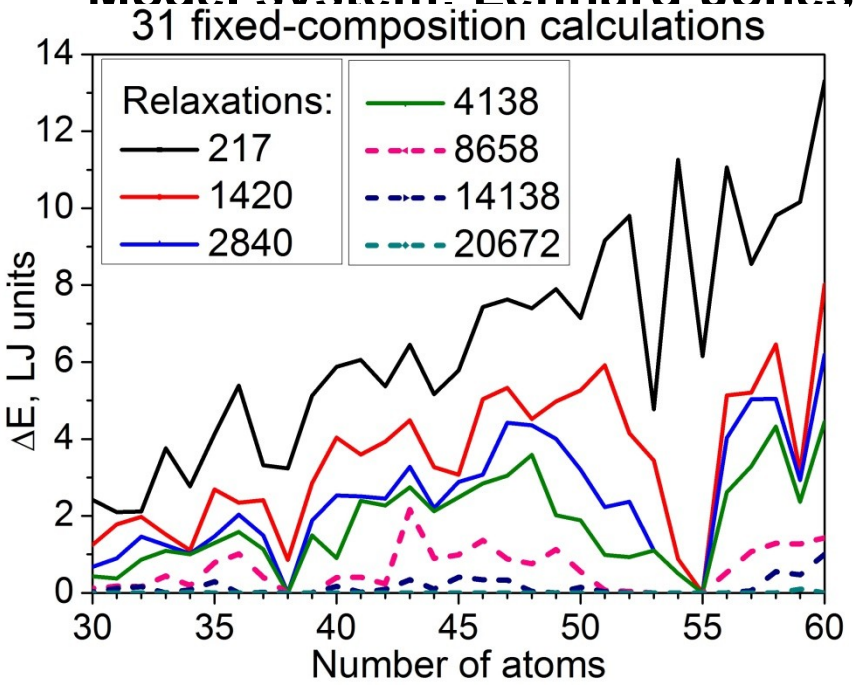

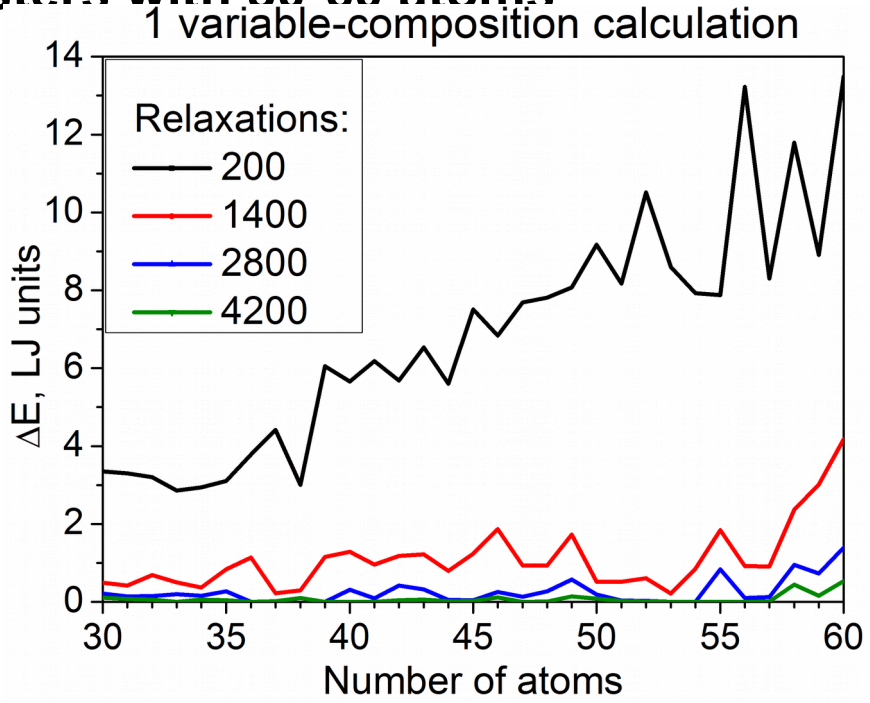

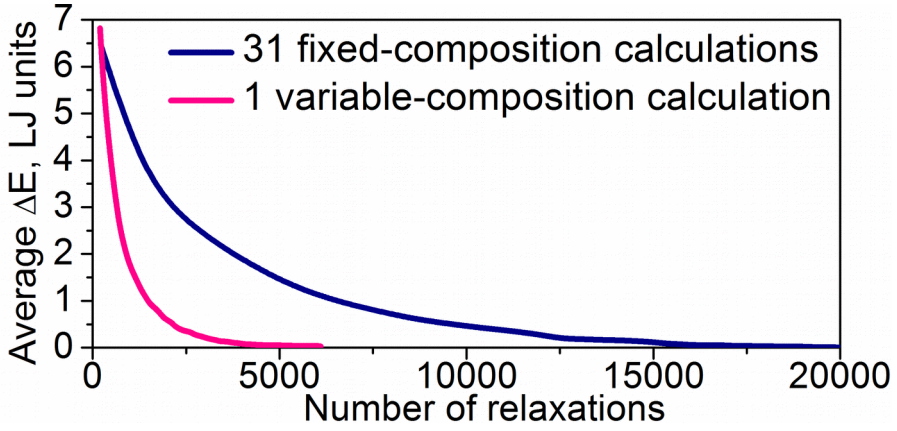

Total number of relaxations:

Fixed-composition method: ~20000

Variable-composition method: ~4000
Speed up is ~5 times

For binary model clusters:
Speed up is up to 50 times

Ab initio study of Si-O clusters

Si-O clusters:

- practical importance in many fields:

- astrophysics: formation of silicates from SiO molecules in a circumstellar space;
- experiments on growth of oxide-coated Si nanowires from gas-phase SiO
- Super-oxided clusters (Si_nO_m, $m>2n$) can manifest biological activity.

- very complicated for structure prediction:

crystalline silica alone has 14 structural forms.

Ground-state structures of Si-O clusters

Si_nO_m clusters, $1 \le n \le 15$, $0 \le m \le 20$ (315 different compositions)

USPEX + VASP

20 best structures for each composition are refined with GAUSSIAN code, B3LYP/6-311+G(2d,p) approach

n \ *m*	0	1	2	3	4	5	6	7	8	9	10	11	12	13	14	15	16	17	18	19	20
1						*	*	*	*	*	*	*	*	*	*	*	*	*	*	*	*
2							*	*	*	*	*	*	*	*	*	*	*	*	*	*	*
3									*	*	*	*	*	*	*	*	*	*	*	*	*
4											*	*	*	*	*	*	*	*	*	*	*
5												+	*	*	*	*	*	*	*	*	*
6														*	*	*	*	*	*	*	*
7							+														
8		*	*	*	*	*	*	+						*	*	*		*	*	*	*
9		*	*	*	*	*	*	*	+					*	*	*	*	*		*	*
10		*	*	*	*	*	*	*	*	+			+	+	*	*	*	*	*	*	
11		*	*	*	*	*	*	*	*	*	+			*	*	*	*	*	*	*	*
12		*	*	*	*	*	*	*	*	*	*			+	*	*	*	*		*	*
13		*	*	*	*	*	*	*	*	*	*	*	+	+	+	*	*	*	*	*	*
14		*	*	*	*	*	*	*	*	*	*	*	*	+	+	+	*	*	*	*	*
15		*	*	*	*	*	*	*	*	*	*	*	*	*	+		+	*	*	*	*

Results:

99 (of 315) clusters – reproduced results of other studies (empty cells);

17 (of 315) clusters – optimal structures were improved (+);

199 (of 315) clusters – were predicted for the first time (*).

Stability of binary clusters

Binary A_nB_m clusters

$$\Delta_{nn}(n,m)=E(n+1,m)+E(n-1,m)-2E(n,m),$$
$$\Delta_{mm}(n,m)=E(n,m+1)+E(n,m-1)-2E(n,m)$$

$$\Delta_{min}(n,m)= \min\{\Delta_{nn}(n,m),\Delta_{mm}(n,m)\}$$

$\Delta_{min}(n,m)<0$ – cluster is unstable

$\Delta_{min}(n,m)>0$ – cluster is stable (magic)

$\Delta_{min}(n,m)$ – numerical degree of stability

Stability map of Si_nO_m clusters: $\Delta_{min}(n,m)$

Regions of instability are marked by blue color.

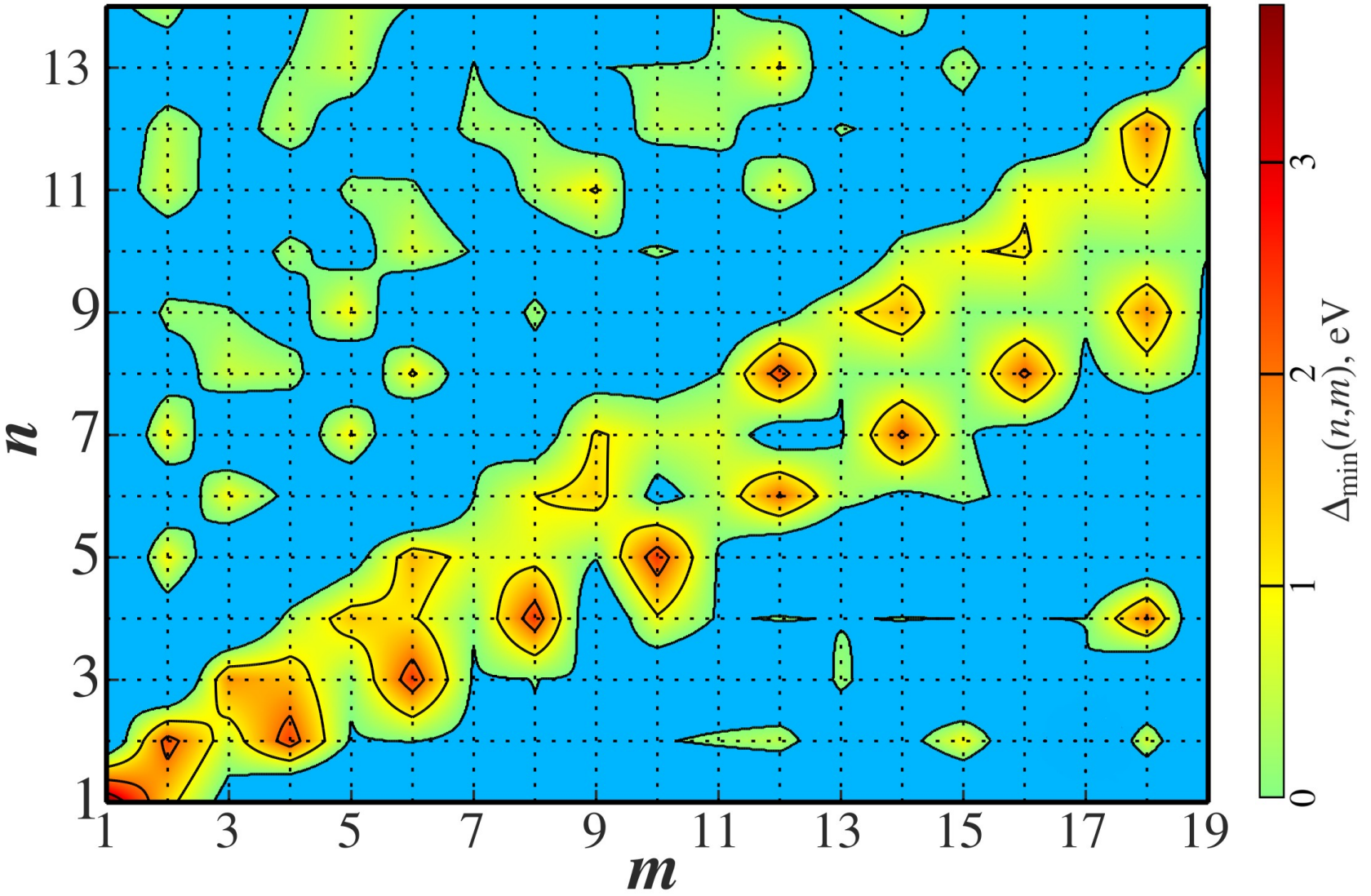

$\Delta_{nn}(n,m)=E(n+1,m)+E(n-1,m)-2E(n,m)$,
$\Delta_{mm}(n,m)=E(n,m+1)+E(n,m-1)-2E(n,m)$

$\Delta_{min}(n,m)= \min\{\Delta_{nn}(n,m),\Delta_{mm}(n,m)\}$

Stability map of Si_nO_m clusters: $\Delta_{min}(n,m)$

Regions of instability are marked by blue color.

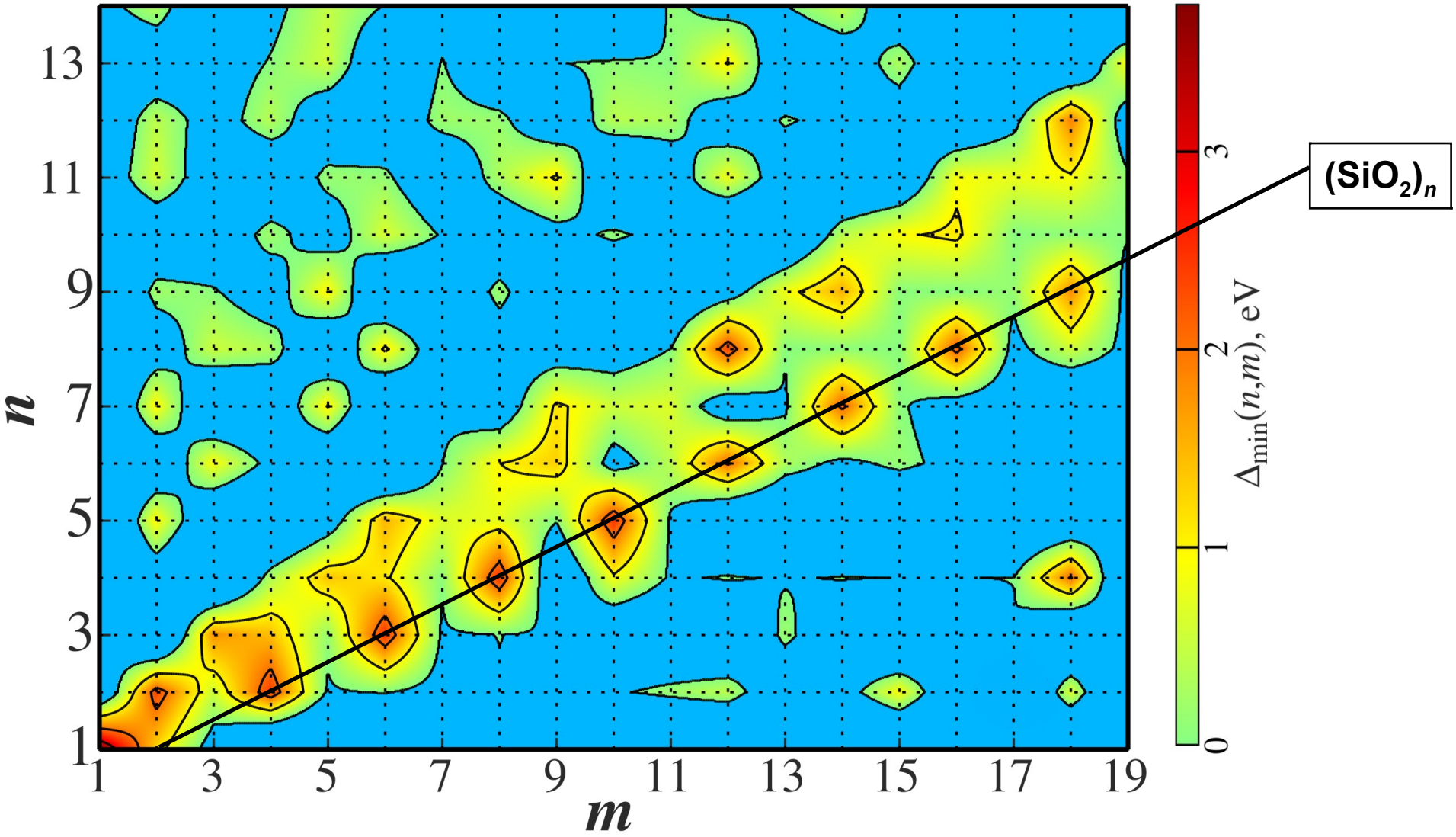

$\Delta_{nn}(n,m)=E(n+1,m)+E(n-1,m)-2E(n,m)$,

$\Delta_{mm}(n,m)=E(n,m+1)+E(n,m-1)-2E(n,m)$

$\Delta_{min}(n,m)= \min\{\Delta_{nn}(n,m),\Delta_{mm}(n,m)\}$

Stability map of Si_nO_m clusters: $\Delta_{min}(n,m)$

Regions of instability are marked by blue color.

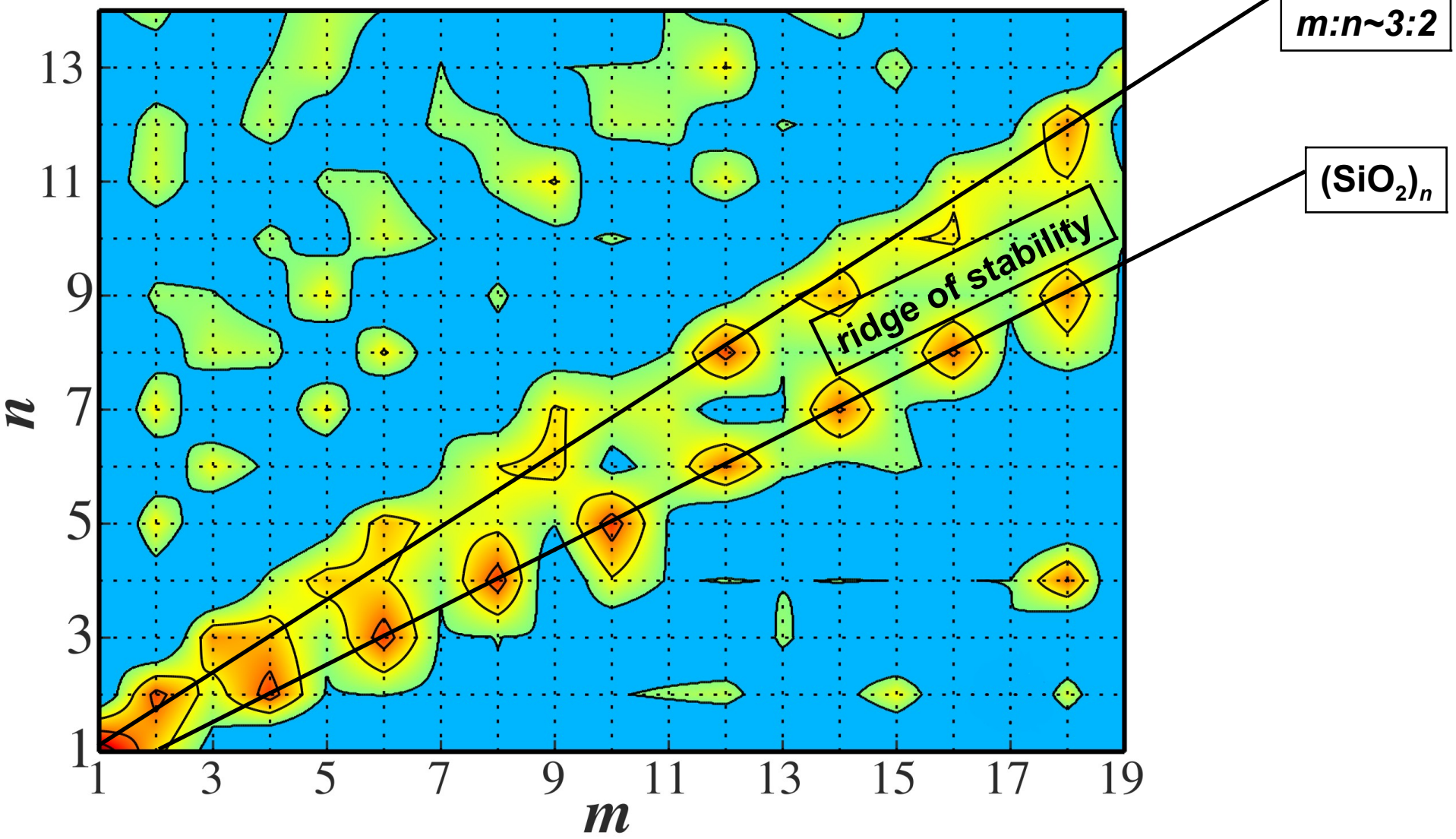

$\Delta_{nn}(n,m)=E(n+1,m)+E(n-1,m)-2E(n,m)$,

$\Delta_{mm}(n,m)=E(n,m+1)+E(n,m-1)-2E(n,m)$

$\Delta_{min}(n,m)= \min\{\Delta_{nn}(n,m),\Delta_{mm}(n,m)\}$

Stability map of Si_nO_m clusters: $\Delta_{min}(n,m)$

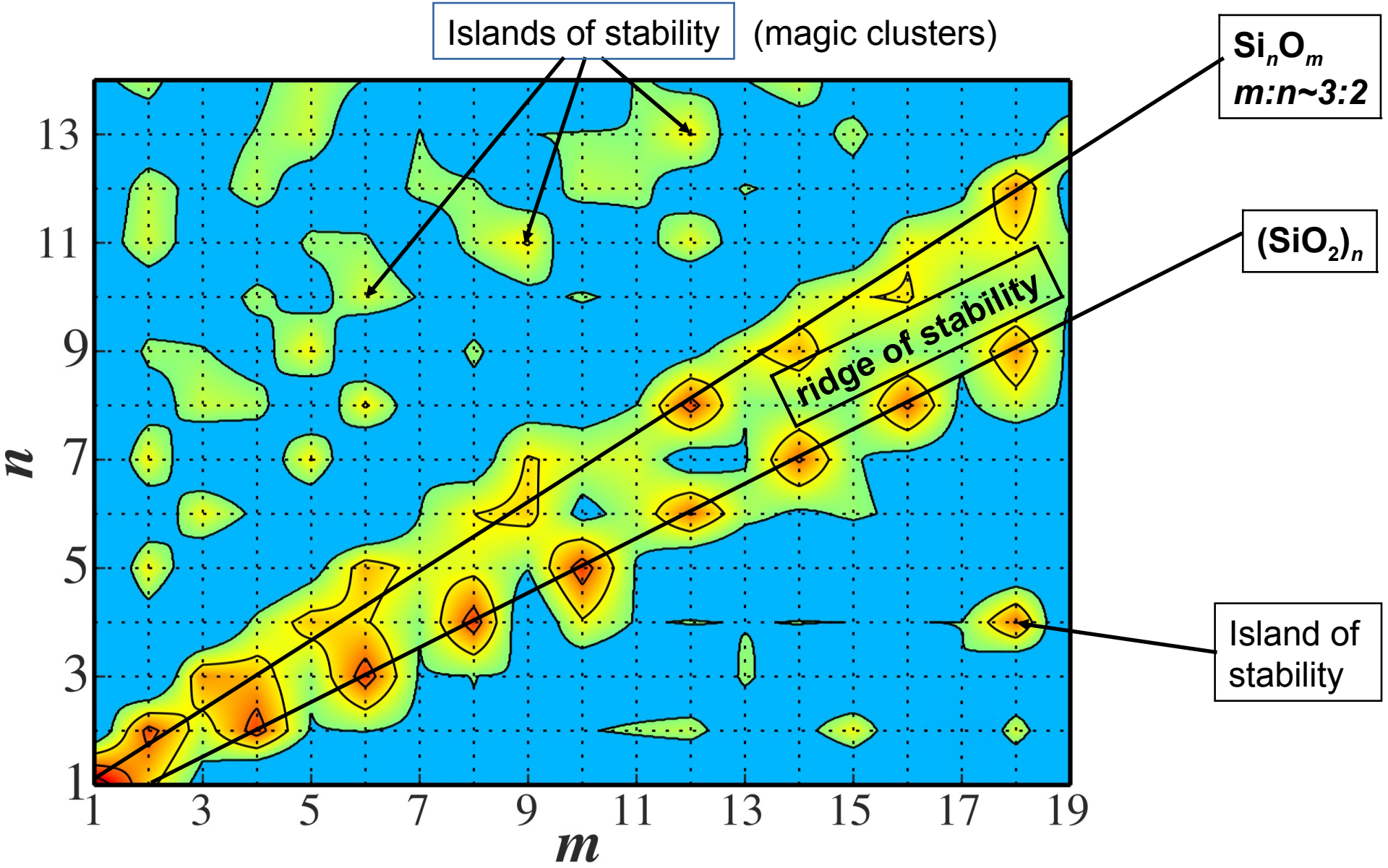

$\Delta_{nn}(n,m)=E(n+1,m)+E(n-1,m)-2E(n,m)$,
$\Delta_{mm}(n,m)=E(n,m+1)+E(n,m-1)-2E(n,m)$

$\Delta_{min}(n,m)= \min\{\Delta_{nn}(n,m),\Delta_{mm}(n,m)\}$

Stability map of Si_nO_m clusters: $\Delta_{min}(n,m)$

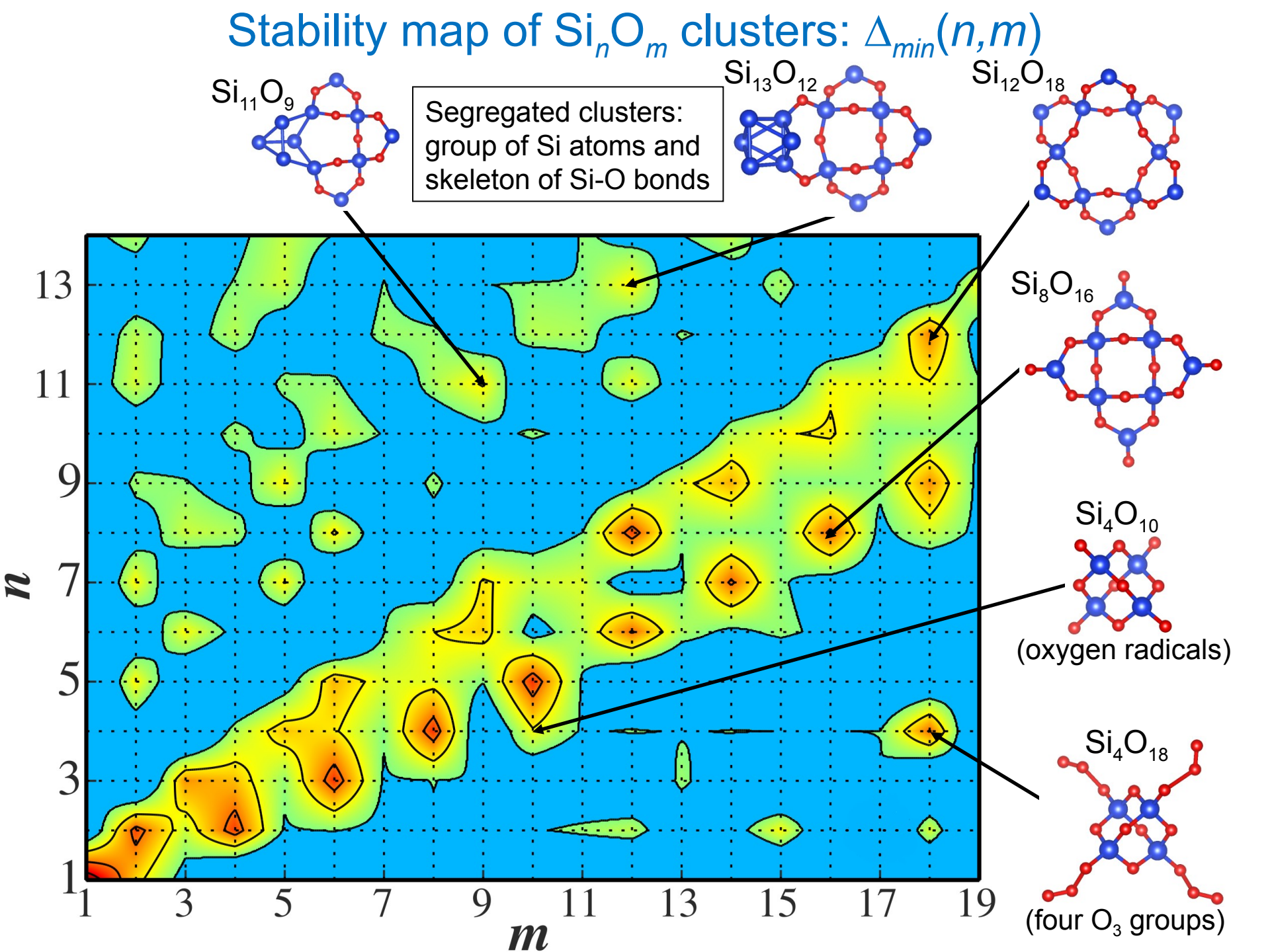

Charge traps in CdSe clusters

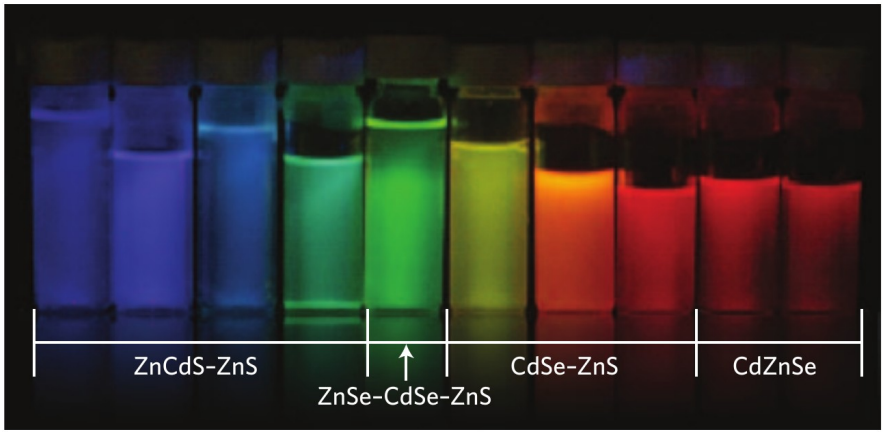

λ depends on cluster size making them perfect candidates for LEDs/dyes, however quantum yield is limited by charge trapping (due to localized surface states)

Charge traps in CdSe clusters

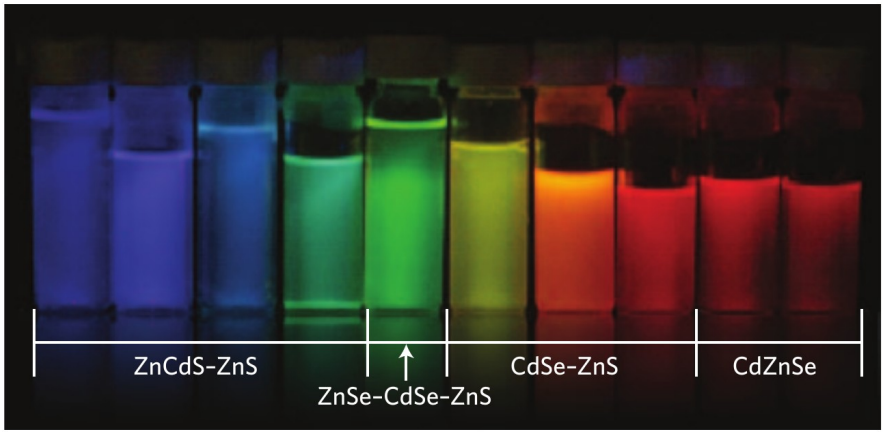

λ depends on cluster size making them perfect candidates for LEDs/dyes, however quantum yield is limited by charge trapping (due to localized surface states)

Solutions:
1. Core-shell structures with dielectric shell
2. Passivation by ligands

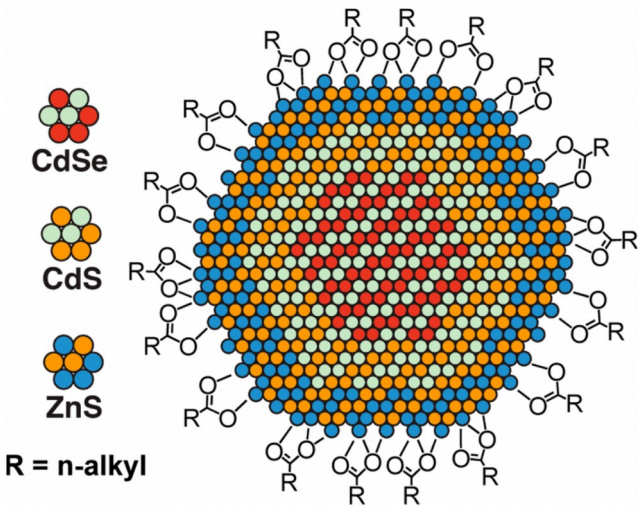

Charge traps in Cd_nSe_m clusters: final picture

To study charge trapping one must inspect the localization of the near-gap electronic states

$$\mathrm{PR}_i = \frac{1}{\sum_a P_{i,a}^2}$$

$P_{i,a}$ – contribution of atom a to i-th MO, $\sum_a P_{i,a} = 1$

These are usually taken via Mulliken population analysis:

$\Psi_i = \sum_i c_{\mu i}\phi_\mu$ i-th MO is expanded over basis set of atomic orbitals φ_μ

$$P_{i,a} = \sum_{\mu \in a} c_{\mu i}^* c_{\nu i} \underbrace{\langle \varphi_\mu | \varphi_\nu \rangle}_{\text{overlap integral}}$$

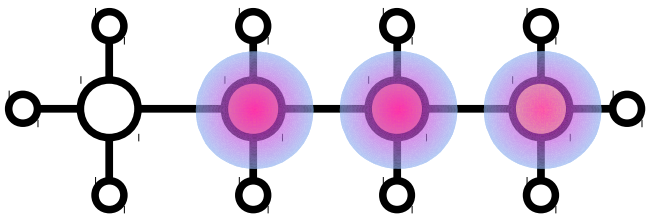

$P_{i,a}$ = 0 = 1/3 =1/3 =1/3

$$\mathrm{PR} = \frac{1}{\frac{1}{9}+\frac{1}{9}+\frac{1}{9}} = 3 \approx N_{\mathrm{loc}}$$

Maps of the localizations in Cd_nSe_m clusters: The higher N/N_{loc} – the more localized state

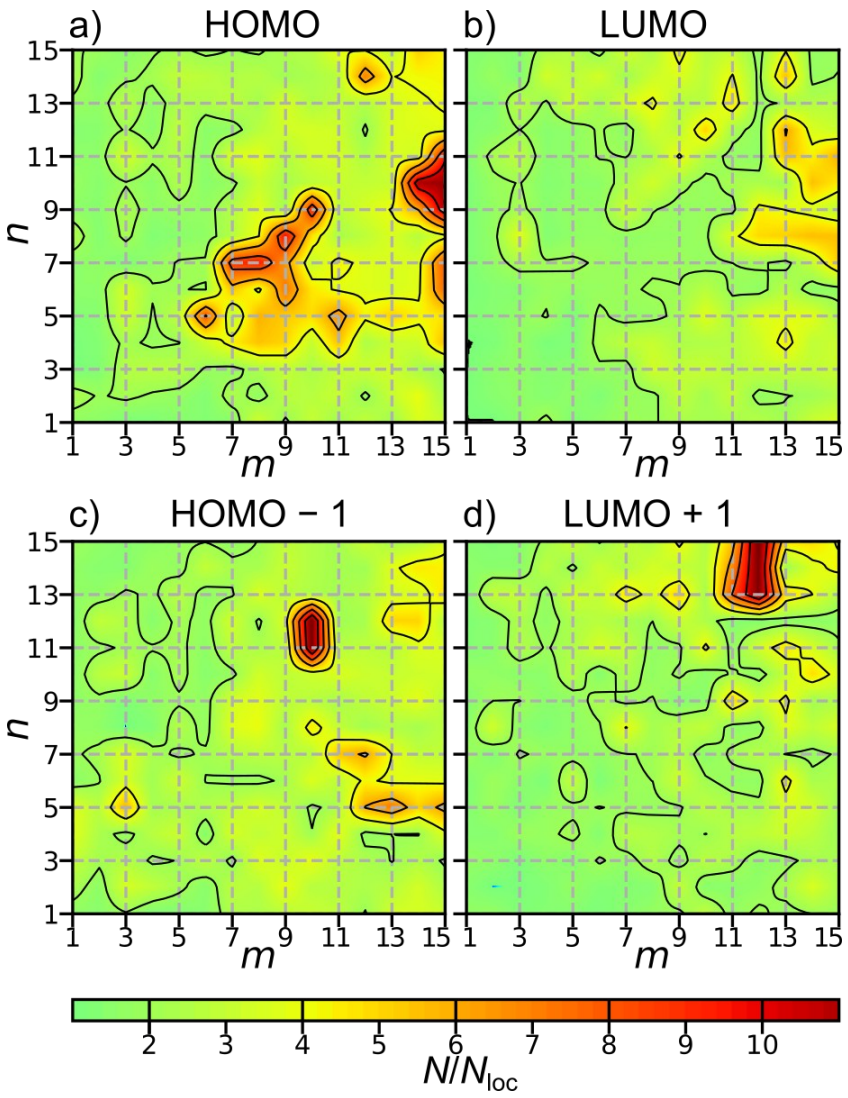

Maps of the localizations in Cd_nSe_m clusters: The higher N/N_{loc} – the more localized state

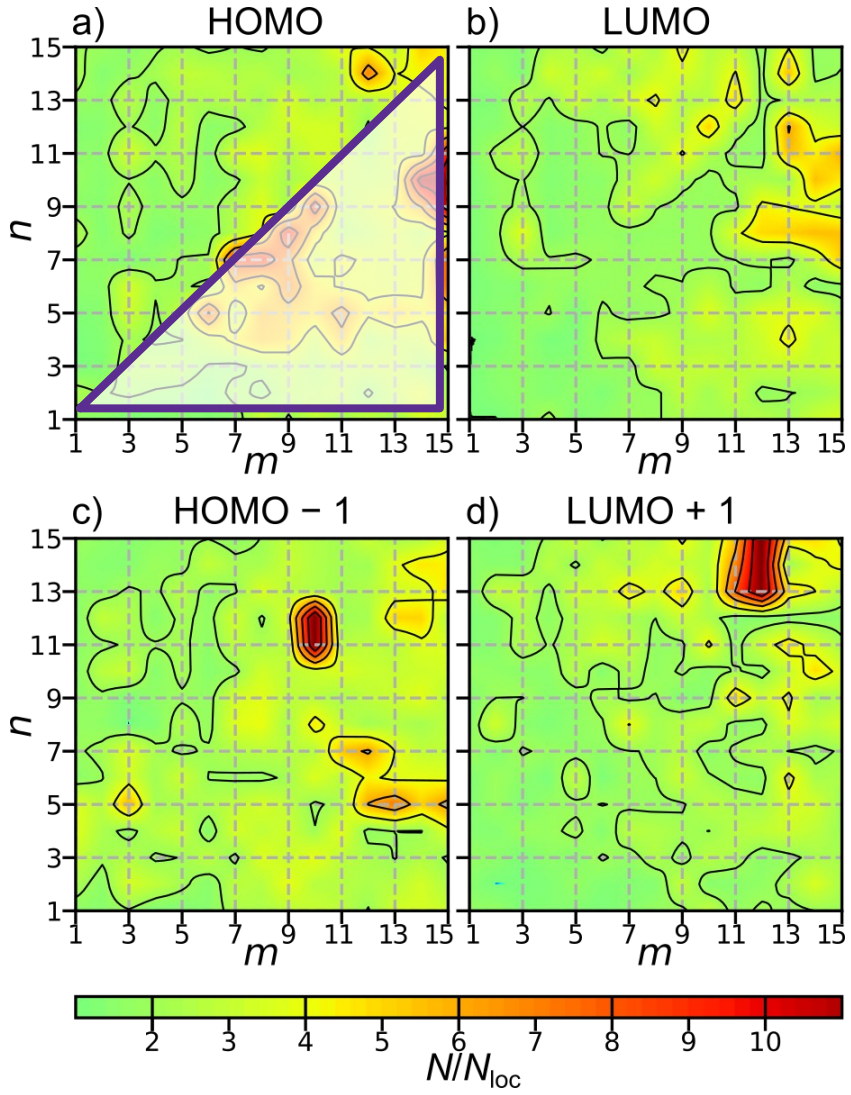

1. Localized states are mostly in lower right triangle – traps are mostly observed in Se-rich clusters

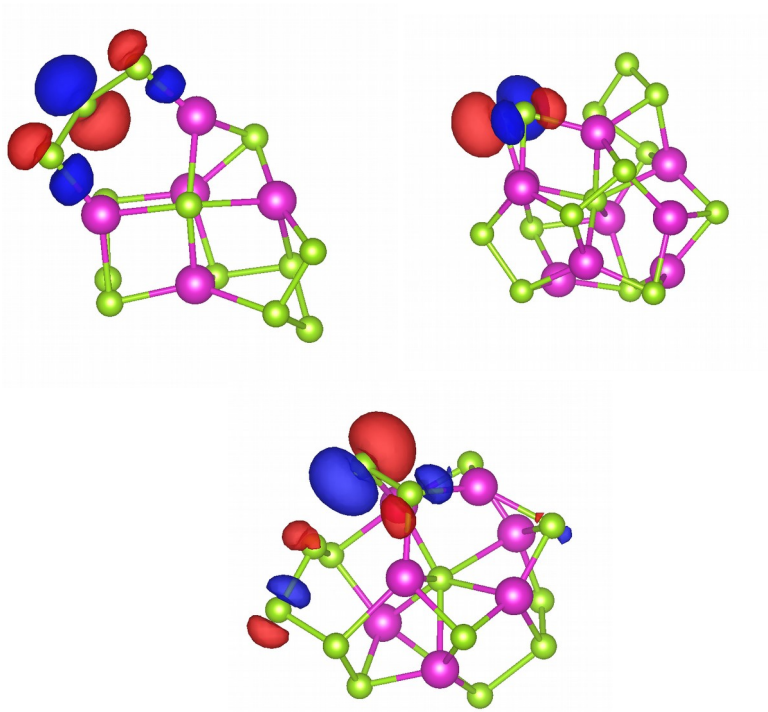

Maps of the localizations in Cd_nSe_m clusters: The higher N/N_{loc} – the more localized state

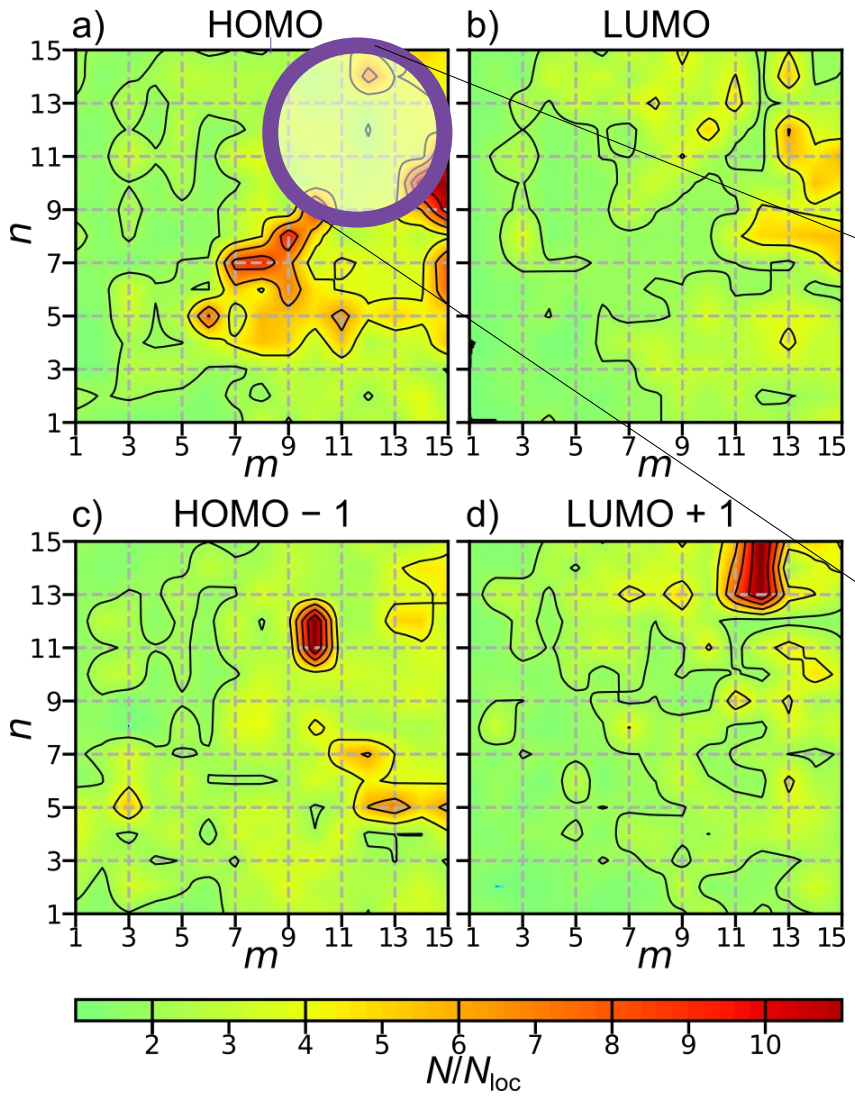

2.Maps are rather **smooth**:

close compositions

▼

close structures

▼

close properties

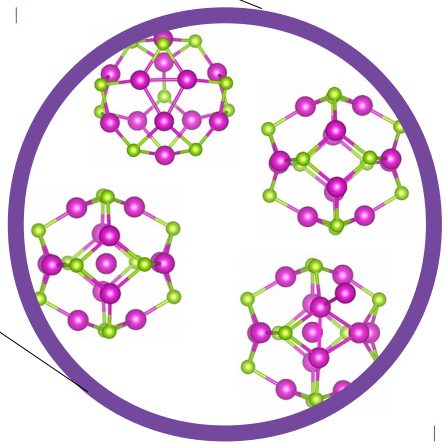

Maps of the localizations in CdnSem clusters: The higher N/N_{loc} – the more localized state

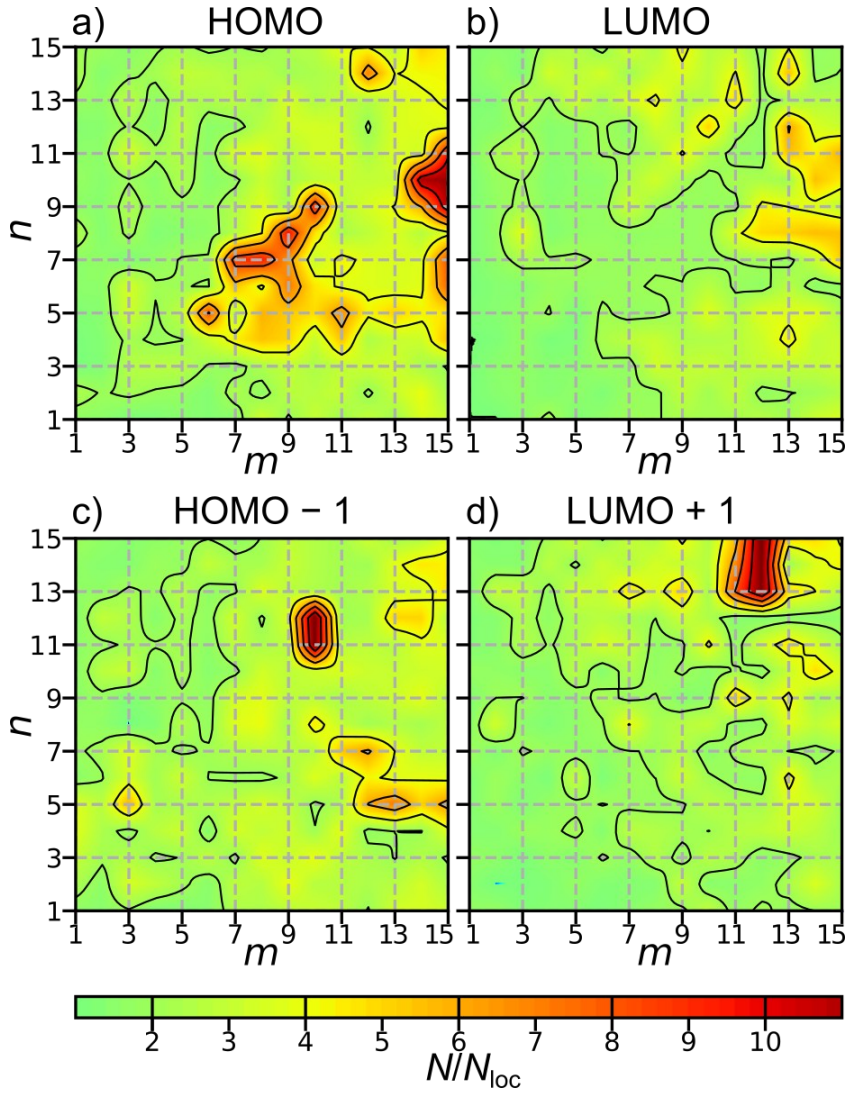

3. Despite the absence of passivating ligands, most clusters are **trap-free**.

Contrary to the previous studies where traps were thought to be inherent to unpassivated crystalline surface.

The reason is the **self-healing effect** due to passivation

Self-healing of traps

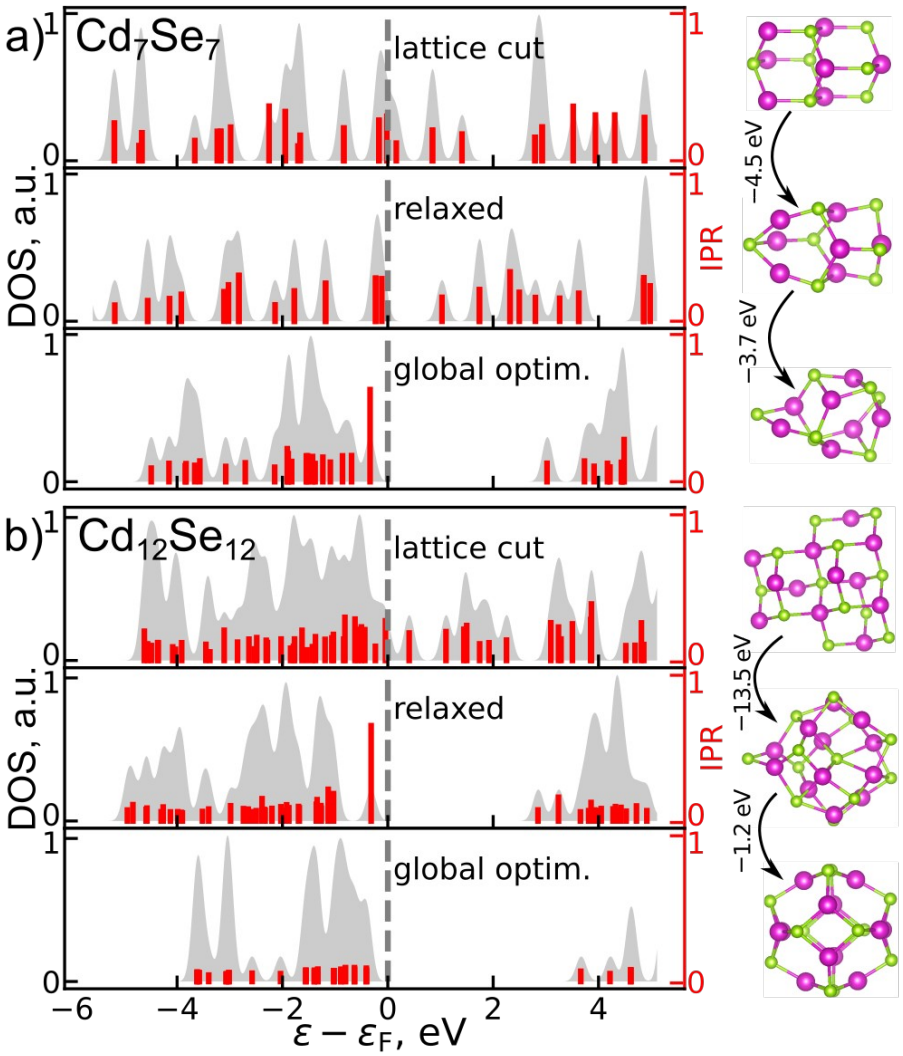

Three stages of stabilization:

1 Cluster is simply cut from a zincblende:

(near-zero gap)

2. Same cluster, relaxed

(opening the gap, mid-gap states are suppressed)

3. Global optimum structure

(gap is wide, no mid-gap states)

Types and mechanisms of trapping

Trap Symbol

Schematic structure of a trap

Example: cluster & trap orbital

$\langle N_{loc} \rangle$ − localization (atoms)

N_{tr} − abundance

T^{I}_{a}(Se p_z)

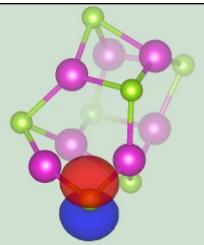

$\langle N_{loc} \rangle$=1.9, N_{tr}=11

Cd_7Se_7 (HOMO)

T^{I}_{b}(Se π*)

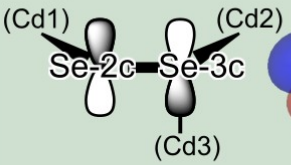

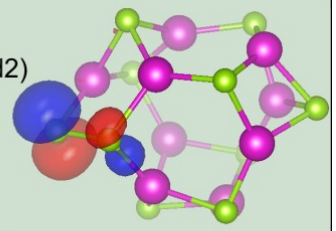

$\langle N_{loc} \rangle$=2.3, N_{tr}=9

Cd_9Se_{10} (HOMO)

T^{I}_{c}(Se π*)

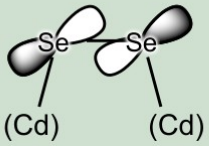

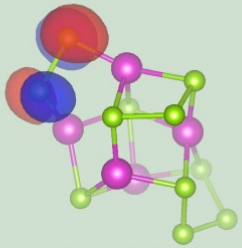

$\langle N_{loc} \rangle$=2.4, N_{tr}=1

Cd_5Se_{11} (HOMO)

T^{I}_{d}(Se π*)

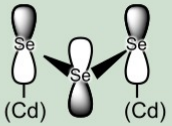

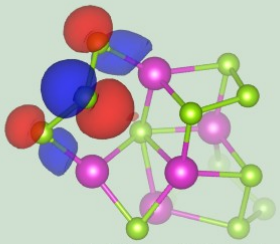

$\langle N_{loc} \rangle$=3.1, N_{tr}=1

Cd_5Se_{13} (HOMO)

T^{I}_{e}(Se π*)

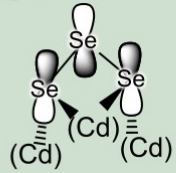

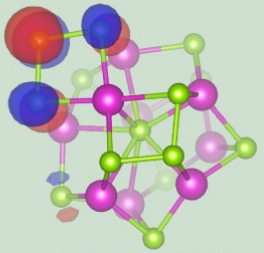

$\langle N_{loc} \rangle$= 3.8, N_{tr}=1

Cd_9Se_{14} (HOMO)

T^{II}_{a}(Se σ*)

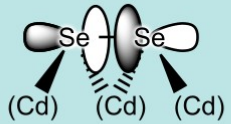

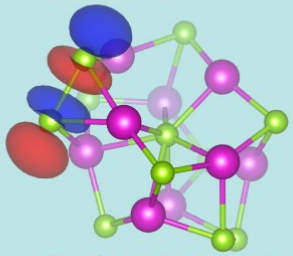

$\langle N_{loc} \rangle$=3.9, N_{tr}=1

Cd_9Se_{11} (LUMO+1)

T^{II}_{b}(Se σ*)

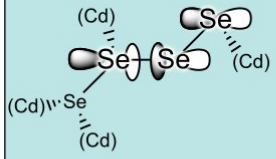

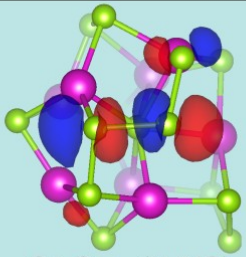

$\langle N_{loc} \rangle$=3.9, N_{tr}=1

Cd_8Se_{14} (LUMO)

T^{III}(Cd@NC)

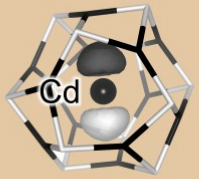

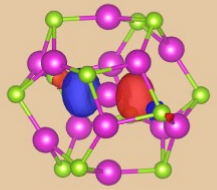

$\langle N_{loc} \rangle$=2.6, N_{tr}=5

$Cd_{13}Se_{12}$ (LUMO+1)

New mechanisms

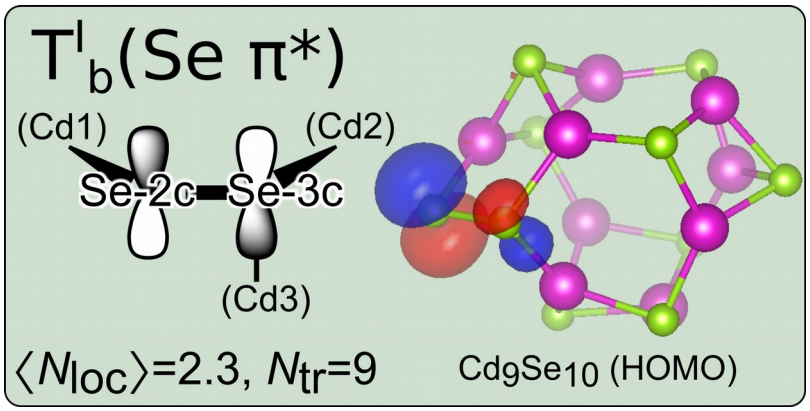

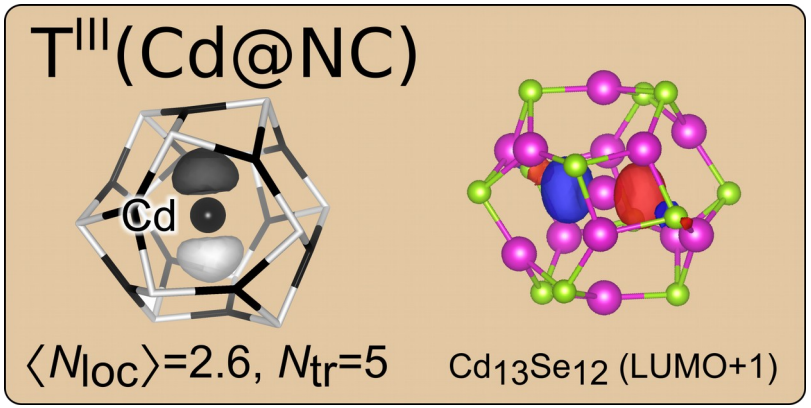

New mechanisms: T^{I}_{b}(Se π*)

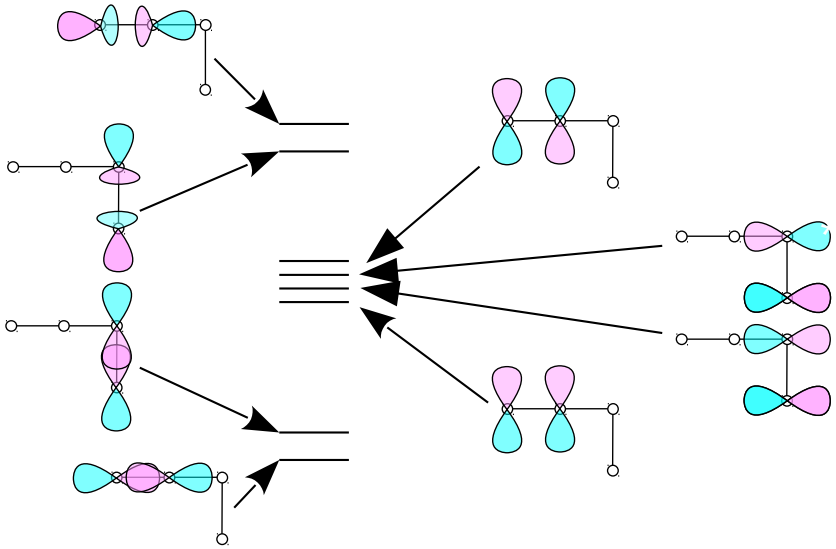

π- and σ-bonding have different energies ($h_\sigma >> h_\pi$

$$\psi_{\pi^*}(\mathbf{r}) \sim \exp\{-d_\sigma|(h_\sigma - h_\pi)2m/\hbar^2|^{1/2}\}$$

Conclusions (CdSe)

1. Electron localization in Cd_nSe_m is inspected in a wide area of compositions (n, m = 1, …, 15)

2. The most widespread traps were find in an unbuased way and classified into three types

3. The corresponding confinement mechanisms are explained at the atomistic level

3. The effect of localization on the HOMO-LUMO gap is investigated

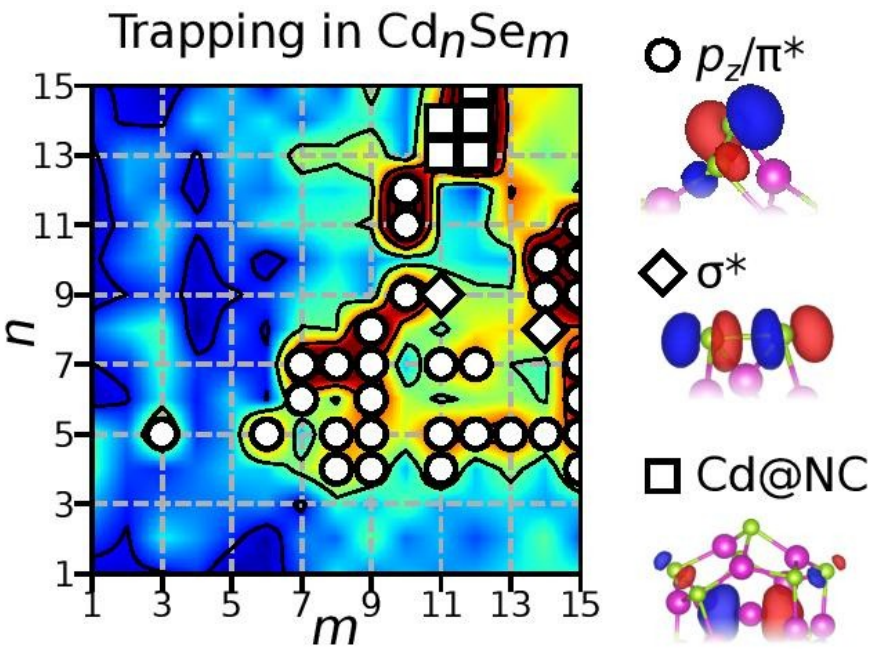

Physical Chemistry Chemical Physics, 2020, DOI: 10.1039/D0CP05139J